Characterization of the transmission resonances in different energy regimes by the multifractal scaling analysis of the electronic transmittance in a one-dimensional random-dimer potential

1997 J. Phys.: Condens. Matter 9 8985

(http://iopscience.iop.org/0953-8984/9/42/013)

J. Phys.: Condens. Matter **9** (1997) 8985–8995. Printed in the UK PII: S0953-8984(97)82100-5

Characterization of the transmission resonances in different energy regimes by the multifractal scaling analysis of the electronic transmittance in a one-dimensional random-dimer potential

Prabhat K Thakur and Tapas Mitra†

S N Bose National Centre for Basic Sciences, Block JD, Sector III, Salt Lake, Calcutta-700091, India

Received 24 February 1997, in final form 14 July 1997

Abstract. A detailed numerical study of electronic transmittance has been carried out to analyse the nature of the metallic behaviour around the dimer site energy. The transmittance versus energy curve exhibits resonance features, i.e. it becomes nearly flat at and around the dimer on-site energy apart from showing other transmission resonances. The spatial variation of the transmittance for energies in the vicinity of the dimer on-site energy shows Bloch-like extended character. For electron energies slightly away from this region, the transmittance shows some oscillation with energy, and the transmission resonances show spatial variation, having fragmented character which may be attributed to the deviation from the typical Bloch-like extended character of the states in the vicinity of the dimer on-site energy. Our multifractal scaling analysis for the normalized transmittance distinguishes the resonances in the two different regimes.

1. Introduction

During recent years, the nature of electronic states and the behaviour of transport in the random-dimer types of potential [2–8] which are not completely random but have some kind of short-ranged correlation have created a lot of interest. Various models of potentials which are neither completely random nor periodic have been studied, and people have claimed that extended states exist [9, 10]. Among all of the models studied so far, the random-dimer model (RDM) has gained special importance since Wu and Phillips [2, 3] claimed that it has a direct connection with the electronic transport of the polyaniline system. It has been shown by many authors that the random-dimer-type impurity potential yields electronic states which are drastically different from those of the random potential (i.e. without any short-range or long-range correlation) [1] where one expects all states to be exponentially localized, except a few exponentially narrow resonances. Here we will recall some important physical aspects related to the RDM, and we will confine our discussion to the context of the Anderson tight-binding model. In the case of the RDM, Anderson's tight-binding Hamiltonian is taken in such a manner that the impurity site energy ϵ_a occurs only in pairs embedded randomly in the host sample having site energy ϵ_b. Dunlop, Wu and Phillips [4] showed that the reflection coefficient of a system containing a single dimer vanishes when the incoming

† Present address: Department of Physics, Ranaghat College, District: Nadia, PO: Ranaghat, West Bengal, India.

0953-8984/97/428985+11$19.50

electron energy becomes the same as the dimer on-site energy, provided that $|\epsilon_a - \epsilon_b| \leqslant 2t$, t being the hopping integral. They also claimed that a number $\sqrt{N}$ of states get extended over the whole sample if it contains N sites. However, Gangopadhyay and Sen [7] claimed that for a system containing randomly placed dimers there are $N^{1/3}$ ballistic states. Datta *et al* [5] claimed that the number of non-scattered states depends also on the dimer on-site energy and its concentration in the chain. In a later publication, Datta *et al* [6] studied the nature of states in a RDM through bandwidth scaling analysis. They claimed that the scaling behaviour of the bandwidths shows that the system contains extended states in the vicinity of the dimer site energy.

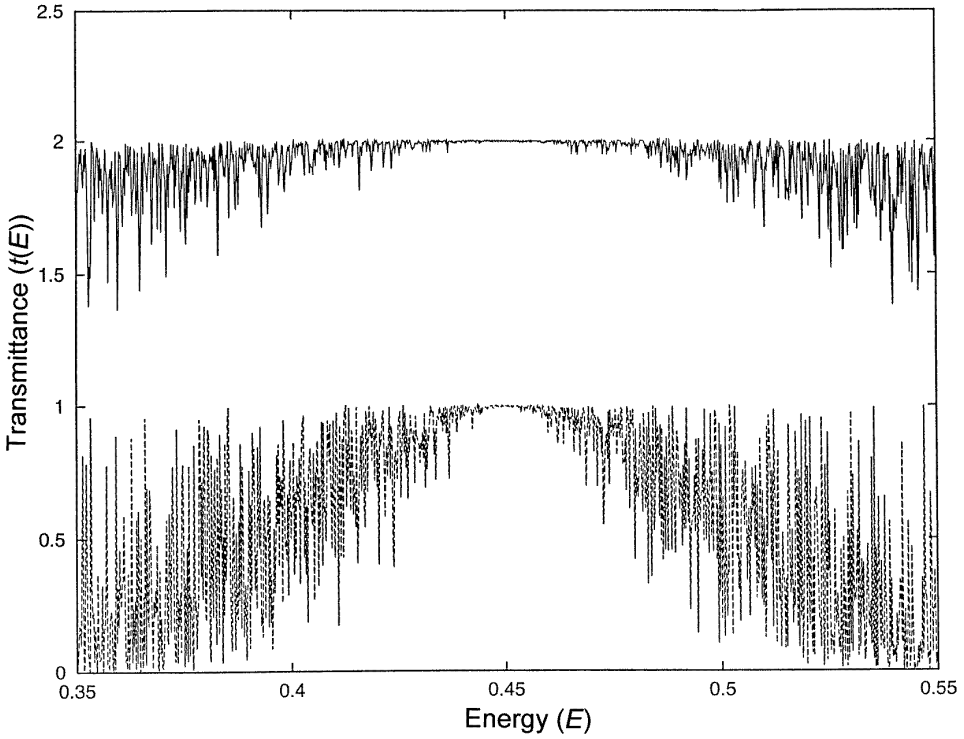

Figure 1. The transmittance (T) versus energy (E) curve for $\epsilon_A = 0.45$ units, $\epsilon_B = 0.145$ units, $c = 0.10$, and $N = 2 \times 10^5$ sites (lower curve), and $N = 2 \times 10^3$ sites (upper curve).

It has been established analytically that the electronic transmittance or wavefunction corresponding to the dimer on-site energy will always satisfy the non-scattering condition, and hence the transmittance will be unity even for an infinitely large system. However, the nature of the electronic transmittance for other energy values has not been analytically established yet. There is still some controversy regarding the nature of the electron delocalization or metallic behaviour around the dimer site energy [6, 7]. Detailed numerical study of the transmittance resonances at different energies may be one possibility for resolving the controversy. Also, we think that in order to understand the electronic transport in the RDM more directly, one should attempt to construct a formalism of multifractal analysis for the normalized electronic transmittance to investigate different states around the dimer on-site energy. It is to be noted that the direct connection between the results that one obtains from the bandwidth scaling analysis for the RDM and the transmittance resonances

for the RDM is not obvious. It should also be noted that the multifractal scaling analysis for the normalized transmittance has been previously successfully performed to make the distinction between critical, extended and localized states in the generalized Aubry model [11] and also to analyse the nature of Azbel resonances in 1-D random potentials [12].

In this communication, the spatial variation of the electronic transmittance has been carefully studied through a multifractal scaling formalism to analyse the nature of the electron delocalization in the immediate vicinity and in a regime which is slightly away from the immediate vicinity. In a previous communication, a distinction between the states at the centre of the plateau region and stochastic resonances far away from the plateau region was made through multifractal scaling analysis [8]. In contrast, in this communication, a distinction is made between different states in the immediate vicinity of the dimer on-site energy and states slightly away from this region. Also, the tight-binding Hamiltonian is used in this communication instead of the arrays of delta-function potential models used in reference [8]. It is to be noted that Wu and Phillips performed a mapping of polyaniline systems onto the tight-binding form of the RDM. In the RDM, delocalization happens at around the impurity site energy. The situation is different in the case of the model considered in reference [8], and the exact relationship between the parameters of the two models is not obvious. Also, most of the work in the field of delocalization induced by dimer-type correlation has been done within the framework of the tight-binding model. So, in our view, characterization of different resonance states in the case of the tight-binding RDM is a matter of immense academic and practical interest.

2. Formalism

2.1. Electronic transmittance in the transfer matrix method

Here we consider the Anderson tight-binding Hamiltonian ($\hat{H}$) with nearest-neighbour interaction:

$$\hat{H} = \sum_i \epsilon_i |i\rangle\langle i| + \sum_{i,j} v_{ij} |i\rangle\langle j| \tag{2.1}$$

where ϵ_i represents the on-site energy at the ith site, and the v_{ij} are the nearest-neighbour tunnelling matrix elements connecting sites i and j.

Now, for the stationary-state solution of the above Hamiltonian corresponding to the energy eigenvalue E, we can write

$$(E - \epsilon_n)C_n = v_{n,n+1}C_{n+21} + v_{n,n-1}C_{n-1} \tag{2.2}$$

where C_n is the probability amplitude that the site n is occupied. Now we consider a situation where the first and the $(N+1)$th sites of a RDM chain are attached to two perfectly conducting semi-infinite leads. Following Liu and Chao [13] and Thakur *et al* [11], we take the site amplitude as

$$C_n = \begin{cases} A_k^+ \mathrm{e}^{\mathrm{i}kn} + A_k^- \mathrm{e}^{-\mathrm{i}kn} & \text{for } n \geqslant (N+1) \\ B_k^+ \mathrm{e}^{\mathrm{i}kn} + B_k^- \mathrm{e}^{-\mathrm{i}kn} & \text{for } n \leqslant 1. \end{cases} \tag{2.3}$$

Then, using the standard transfer matrix procedure, one can connect the incoming and outgoing solutions as follows:

$$\begin{bmatrix} A_k^- \\ A_k^+ \end{bmatrix} = \mathbf{T}(k_j N) \begin{bmatrix} B_k^- \\ B_k^+ \end{bmatrix} \tag{2.4}$$

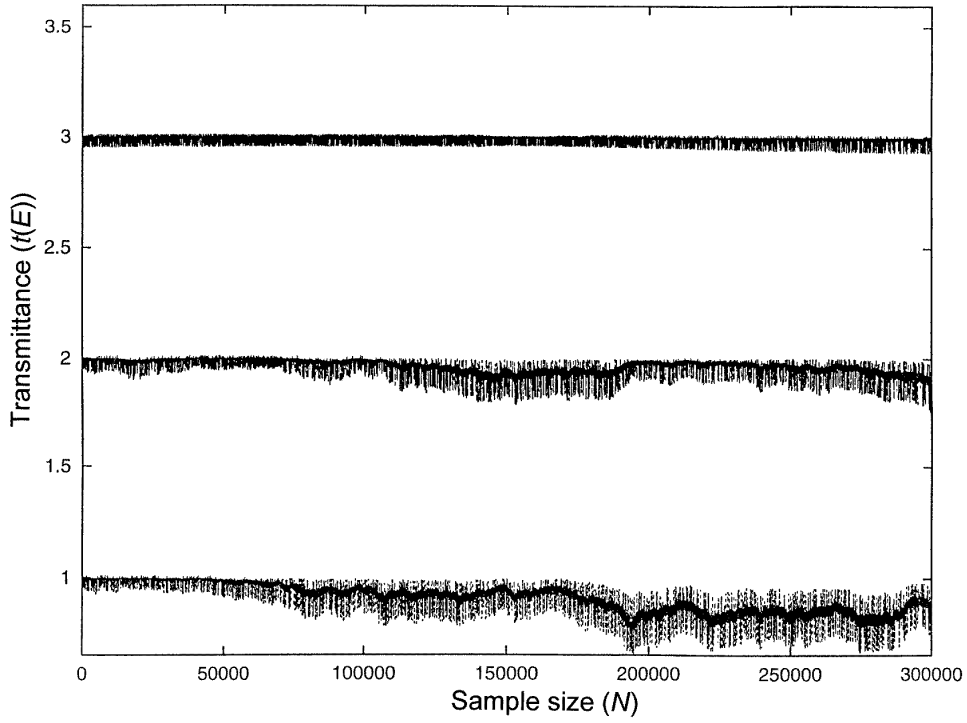

Figure 2. The transmittance (T) versus sample size (N) curve for $E = 0.452\,28$ units (topmost curve), $E = 0.472\,16$ units (middle curve), and $E = 0.471\,920$ units (lowest curve) for the same set of parameters as for figure 1.

where

$$\mathbf{T}(k; N) = \begin{bmatrix} e^{ik(N+1)} & 0 \\ 0 & e^{-ik(N+1)} \end{bmatrix} \left(\mathbf{S}^{-1} \prod_{i=1}^{N+1} \mathbf{P}_i \mathbf{S} \right) \tag{2.5}$$

and

$$\mathbf{S} = \begin{bmatrix} e^{-ik} & e^{ik} \\ 1 & 1 \end{bmatrix} \tag{2.6}$$

and

$$\mathbf{P}_i = \begin{bmatrix} (E - \epsilon_i)/t & -1 \\ 1 & 0 \end{bmatrix}. \tag{2.7}$$

Now, to calculate the transmittance, we take A_k^- to be zero. The reflectance can be obtained from

$$r(E, N) = \left| \frac{B_k^-}{B_k} \right|^2$$

and the transmittance t from the relation $t(E, N) = 1 - r$.

2.2. Multifractal scaling analysis of the normalized transmittance

We will discuss only the multifractal scaling algorithm developed by Chabra and Jensen [15]. This algorithm has been used in analysing the crossover states in the generalized

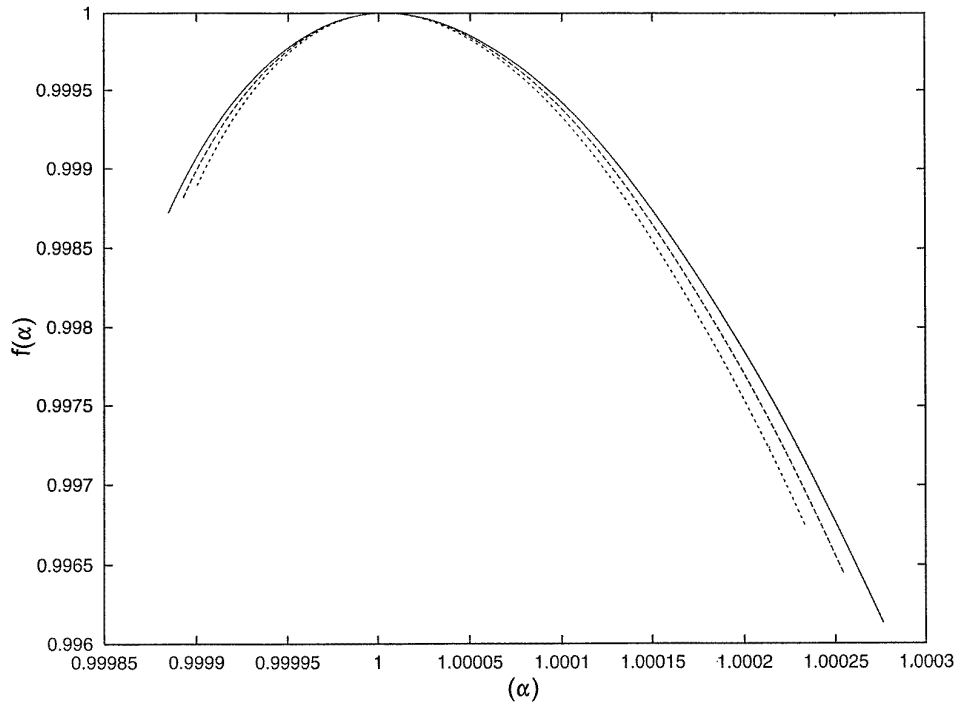

(a)

Figure 3. (a) The $f(\alpha)$ versus α curve for the same set of parameters as for figure 1, but for $E = 0.452\,28$ units, with the corresponding system sizes being $N = 5 \times 10^4$ sites (bold line), $N = 1 \times 10^5$ sites (dashed line), $N = 2 \times 10^5$ sites (dotted line). (b) The $f(\alpha)$ versus α curve for the same set of parameters as for figure 1, but for energy $E = 0.472\,16$ units, with the corresponding system sizes being $N = 1.5 \times 10^5$ sites (dotted line), $N = 2 \times 10^5$ sites (dashed line), and $N = 3 \times 10^5$ sites (bold line). (c) The $f(\alpha)$ versus α curve for the same set of parameters as for figure 1, but for energy $E = 0.471\,920$ units, with the corresponding system sizes being $N = 1.0 \times 10^5$ sites (dotted line), $N = 1.5 \times 10^5$ sites (dashed line), and $N = 2.5 \times 10^5$ sites (bold line).

Aubry model [11] and in many contexts in the literature [16]. The multifractal formalism has been developed essentially to describe the statistical properties of some measure in terms of its distribution-of-singularity spectrum $f(\alpha)$ corresponding to its singularity strength α [14]. Here we take the normalized transmittance as the measure given by

$$p_i = T_i \Big/ \sum_{i=1}^{N} T_i$$

where T_i is the transmittance from one end of the chain up to the ith segment when the length of the chain is divided into N equal segments such that transmittance for a given size is obtained by always increasing the previous size by adding the same number of atoms. According to Chabra and Jensen [15], if one defines the Qth moment of the probability measure by the following expression:

$$\mu_i(Q; N) = p_i^Q \Big/ \sum_{i=1}^{N} p_i^Q$$

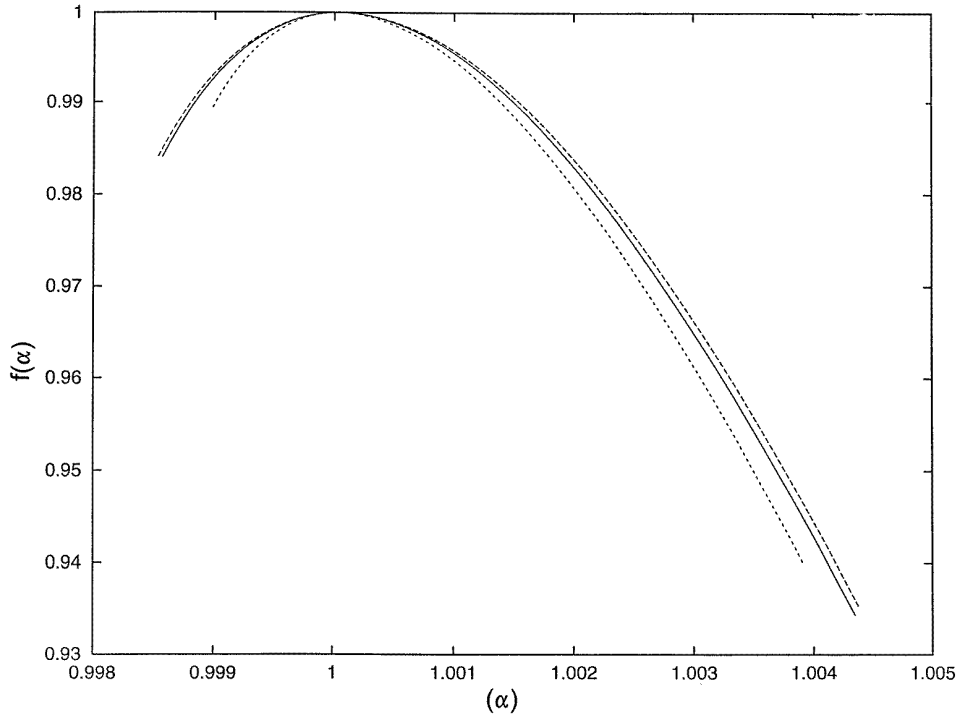

(b)

Figure 3. (Continued)

then a complete characterization of the fractal singularities can be made in terms of this function. Hence one can derive the spectrum of the fractal singularities defined by $\{\alpha, f(\alpha)\}$, where α characterizes the strength of the type of singularity and $f(\alpha)$ the fractal dimension of the set on which singularities of this type are defined. Then the expression for $f(\alpha)$ as suggested by Chabra and Jensen is the following:

$$f(\alpha) = \lim_{N\to\alpha} -\frac{1}{\ln N}\sum_{i=1}^{N}\mu_i(Q,N)\ln\mu_i(Q,N)$$

and the corresponding strengths α of the singularities are obtained as

$$\alpha = \lim_{N\to\alpha} -\frac{1}{\ln N}\sum_{i=1}^{N}\mu_i \ln p_i.$$

In this formalism, one need not calculate the generalized D_Q which corresponds to the scaling exponents for the Qth moments of the measure. The old formalism for determining $f(\alpha)$ from the Legendre transform of the $Q-1$ versus D_Q curve involves a numerical operation which has several disadvantages, like missing real discontinuities leading to phase transitions.

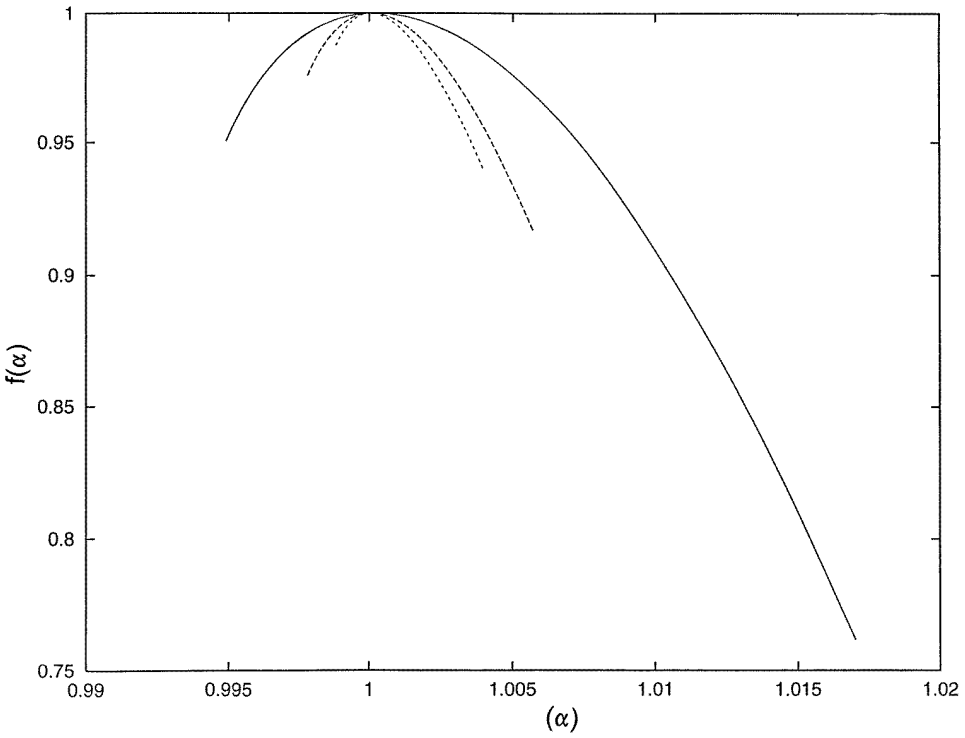

(c)

Figure 3. (Continued)

3. Results and discussion

In our numerical work, we have considered the hopping parameter to be unity in the lead as well as in the sample, and all other energy parameters have been considered in units of unit hopping throughout the calculations. Firstly, we numerically compute the electronic transmittance for a chain having the dimer on-site energy $\epsilon_A = 0.45$ units, and the host site energy $\epsilon_B = 0.145$ units, the concentration c of the dimer impurity being 0.10 for two different system sizes. The transmittance $T(E)$ versus energy (E) plot for $N = 2 \times 10^4$ sites is shown as the upper curve in figure 1. The lower curve shows the transmittance $T(E)$ versus energy E plot for a larger size—$N = 2 \times 10^5$ sites. Here, due to the increase of the system size, we see that the energy region around the dimer site energy over which the transmittance $T(E)$ is nearly flat and almost forms a plateau shrinks.

We have analysed the spatial characteristics of the transmittance in the vicinity of the dimer on-site energy and have gradually crossed these nearby energies to establish whether the behaviour of the spatial form of the transmittance changes from the behaviour in the immediate vicinity. We have shown this by plotting the transmittance $T(E)$ for different lengths for these energy values in figure 2. The top curve shows the transmittance versus length plot for the transmission resonance at $E = 0.452\,28$ units. The middle curve is the same plot but for the resonance state at $E = 0.472\,16$ units, i.e. the energy value is chosen

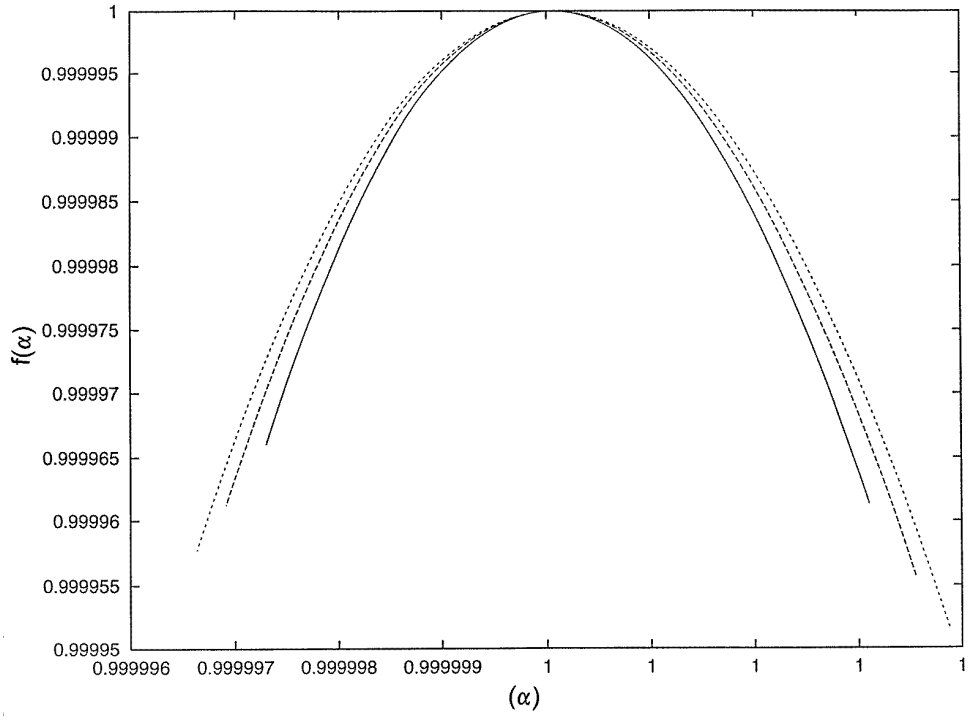

(a)

Figure 4. (a) The $f(\alpha)$ versus α curve for $\epsilon_A = 0.15$ units, $\epsilon_B = 0.045$ units, $c = 0.15$ units, $E = 0.152\,46$ units, and for system sizes $N = 5 \times 10^4$ sites (dotted line), $N = 10^5$ sites (dashed line), and $N = 2.5 \times 10^5$ sites (bold line). (b) The $f(\alpha)$ versus α curve for the same set of parameters as in (a) but for the energy value $E = 0.189\,92$ units and for system sizes $N = 5 \times 10^4$ sites (dotted line), $N = 10^5$ sites (dashed line), and $N = 3 \times 10^5$ sites (bold line).

slightly away from the immediate vicinity, where one can see some changes, and a new pattern starts showing up. The lowest curve shows the variation of the transmittance $T(E)$ with length (N) for $E = 0.471\,920$ units. It is to be noted that the value of the transmittance for $E = 0.471\,92$ units is lower than that for the energy value $E = 0.472\,16$ units. One can think of this energy region as being a physically different region, where a new pattern in the transmittance versus length plot emerges, as compared to the region immediately around the dimer on-site energy. We have performed a multifractal scaling analysis, i.e. produced an $(\alpha, f(\alpha))$ plot, for these states, as described below.

In figure 3(a) the $f(\alpha)$ versus α plot is shown for $E = 0.452\,28$ units; it was produced by choosing three different system sizes: $N = 5 \times 10^4$, 10^5 and 2×10^5 sites. One can notice that with the increase of the system size, the $f(\alpha)$ versus α curves contract systematically. This is a clear signature of a Bloch-like extended state.

In figure 3(b), we have shown an $f(\alpha)$ versus α curve for $E = 0.472\,16$ units and for $N = 1.5 \times 10^5, 2 \times 10^5$, and 3×10^5 sites, where we see that both the $\alpha_{\min}$- and $\alpha_{\max}$-values are now increased in magnitude, but it does not show any definite trend of either a contraction or a systematic increase with system size. However, the $\alpha_{\min}$-values do not change significantly. Here clearly the $\alpha, f(\alpha)$ spectrum signifies the deviation from both the typical Bloch-like extended character and from the exponentially localized nature. In

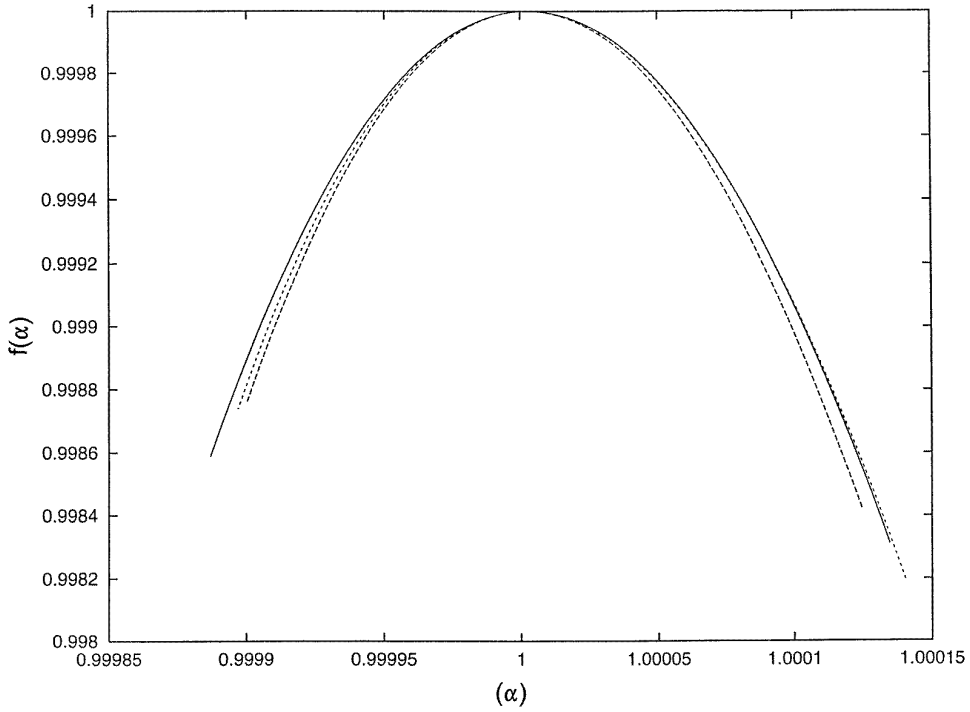

(b)

Figure 4. (Continued)

this sense, this is a region that is physically different from the immediate vicinity, where the Bloch-like extended character is observed.

In figure 3(c), we have shown the plot of $f(\alpha)$ versus α for $E = 0.471\,920$ units and for $N = 1.0 \times 10^5$, 1.5×10^5, and 2.5×10^5 sites, where with the increase of the system size, a tendency towards localization is observed. Here the exponents α and $f(\alpha)$ do not deviate much from unity, and this is a manifestation of a slow electronic localization in the neighbourhood of the actual resonance.

Next, we consider the case where the impurity site energy $\epsilon_A = 0.15$ units, and $\epsilon_B = 0.045$ units, and the impurity concentration $c = 0.15$. In figure 4(a), the $f(\alpha)$ versus α plot has been shown for the energy value $E = 0.152\,40$ units and for three different system sizes, i.e. $N = 5 \times 10^4$, 10^5, and 2.5×10^5 sites. One can clearly see that with the increase of the system size the curves systematically contract.

Now, if one carefully analyses another set of $f(\alpha)$ versus α curves as shown in figure 4(b) for the resonance state at $E = 0.189\,92$ units for three system sizes, $N = 5 \times 10^4$, 10^5, and 3×10^5 sites, one can notice that the curves do not systematically contract, but on the other hand the α_{max}- and α_{min}-values show small oscillations. In this situation, the values of α and $f(\alpha)$ are not very different from unity, and the deviation from the Bloch-like extended character is much less as compared to the resonance state shown in figure 3(b). This is due to the choice of a smaller difference of ϵ_A and ϵ_B, i.e. the on-site energies of the dimer and the host, so the values of transmittance are always relatively high, i.e. closer to unity. Note that all of these resonances are characterized by finite energy widths as compared to the exponentially narrow Azbel resonances.

4. Summary and conclusion

Our numerical study of the electronic transmittance corresponding to the transmission resonances both in the vicinity of the dimer on-site energy and slightly away from it brings into focus important physical aspects which have not been properly investigated before. The transmission resonances for energies very close to the dimer on-site energy exhibit extended character similar to that of Bloch-type wavefunctions. There are also other resonances of finite width away from this region for which the spatial variation of the transmittance exhibits a strongly fluctuating pattern which persists up to a very large system size.

Although Gangopadhyay and Sen [7] observed the existence of these two regions, they did not attempt any rigorous numerical analysis to distinguish the two. Also, in contrast to their speculation that the nearby states will behave like critical states under multifractal analysis, we find a Bloch-like extended character for these states by the same analysis. We claim that the spatial behaviour of the electronic transmittance for energies slightly away from the immediate vicinity is different from that of both Bloch-like extended states and exponentially localized solutions and also from that of exponentially narrow Azbel resonances.

According to Wu, Goff and Phillips [17], any physical system such as conducting polymers or semiconductor heterostructures that can be described by the RDM should exhibit transmission resonances and a drastic enhancement in its conductivity when the Fermi level coincides with the position of the resonance states. We believe also that the transmission resonances where the transmittance shows a behaviour different both from Bloch-like extended states and from exponentially localized wavefunctions may cause enhancement of the conductivity in such systems.

Acknowledgments

P K Thakur would like to thank the S N Bose National Centre for Basic Sciences for financial support. T Mitra would like to thank CSIR of India for financial support in the form of a Senior Research Fellowship.

References

[1] Mott N F and Twose W D 1961 *Adv. Phys.* **10** 107
Borland R E 1961 *Proc. Phys. Soc.* **77** 705
Borland R E 1961 *Proc. Phys. Soc.* **78** 926
Borland R E 1963 *Proc. R. Soc.* A **274** 529
Borland R E 1964 *Proc. Phys. Soc.* **83** 1027
Ishii K 1973 *Prog. Theor. Phys. Suppl.* **53** 77
Ramakrishnan T V and Lee P A 1985 *Rev. Mod. Phys.* **57** 287
[2] Wu H L and Phillips P 1991 *Phys. Rev. Lett.* **66** 1366
[3] Phillips P and Wu H L 1991 *Science* **252** 1805
[4] Dunlop D, Wu H L and Phillips P 1990 *Phys. Rev. Lett.* **65** 88
[5] Datta P K, Giri D and Kundu K 1993 *Phys. Rev.* B **47** 10 727
[6] Datta P K, Giri D and Kundu K 1993 *Phys. Rev.* B **48** 16 347
[7] Gangopadhyay S and Sen A K 1992 *J. Phys.: Condens. Matter* **4** 9939
[8] Basu C and Thakur P K 1995 *Physica* A **217** 2 89
[9] Macia E and Dominguiz Adame F 1996 *Phys. Rev. Lett.* **76** 2957
[10] Chakraborti A, Karmakar S and Moitra R K 1995 *Phys. Rev. Lett.* **74** 1403
[11] Thakur P K, Basu C, Mookerjee A and Sen A K 1992 *J. Phys.: Condens. Matter* **4** 6095
[12] Azbel M Ya and Soven P 1983 *Phys. Rev.* B **27** 831

Basu C, Mookerjee A, Sen A K and Thakur P K 1991 *J. Phys.: Condens. Matter* **3** 9055
[13] Liu Youyan and Chao K A 1986 *Phys. Rev.* B **34** 5247
[14] Halsey T C, Jensen M H, Kadanoff L P, Procacia I and Shraiman B I 1986 *Phys. Rev.* A **33** 1141
[15] Chabra A and Jensen R V 1989 *Phys. Rev. Lett.* **62** 1327
[16] Mandelbrot B B, Evertsz C J G and Hayakawa Y 1990 *Phys. Rev.* A **42** 4528
Coutinho S, Donato Neto O, de Almeida J R L, Curado E M F and Morgado W A M 1992 *Physica* A **185** 271
Morgado W A M, Coutinho S and Curado E M F 1990 *J. Stat. Phys.* **61** 913
Freitas A D and Coutinho S 1993 *Fractals* **1** 694
[17] Wu H L, Goff W and Phillips P 1992 *Phys. Rev.* B **45** 1623